Titania Nanostructured Films Derived from a Titania Nanosheet/Polycation Multilayer Assembly via Heat Treatment and UV Irradiation

Takayoshi Sasaki,* Yasuo Ebina, Katsutoshi Fukuda, Tomohiro Tanaka, Masaru Harada, and Mamoru Watanabe

Advanced Materials Laboratory, National Institute for Materials Science, 1-1 Namiki, Tsukuba, Ibaraki 305-0044, Japan

Received March 6, 2002. Revised Manuscript Received June 17, 2002

A multilayer film of titania nanosheet crystallites and poly(diallyldimethylammonium chloride) has been modified via heat treatment or exposure to UV light. The resulting films in various chemical compositions and crystal structures have been characterized by X-ray diffraction, FT-IR spectroscopy, X-ray photoelectron spectroscopy, and spectroscopic ellipsometry. Thermal or photocatalytic decomposition of polycations in the nanosheet gallery was achieved by heating to 400 °C or UV irradiation, respectively, which produced inorganic multilayers composed of the nanosheets and charge-balancing cations such as ammonium and/or oxonium ions. The polycation removal brought about an improvement in the multilayer stacking order, accompanied by a decrease in inter-nanosheet distance by ∼35%. The nanosheet architecture as well as multilayer structure collapsed upon heating at 500 °C or higher, yielding ultrathin films of TiO_2 (anatase and then rutile). The films exhibited a wide range of optical and photochemical properties dependent on modifications.

Introduction

Intensive research activities have been conducted recently on the fabrication of titania thin films, motivated by their useful applications such as optical coating, photocatalytic decomposition of pollutants, and solar energy conversion.[1] A number of synthetic approaches including sol−gel processing,[2] chemical vapor deposition,[3] and sputtering[4] have been employed for the preparation of titania films. Recently, a variety of new low-temperature routes, which allow the architecture of films to be tailored on a nanometer scale, have been developed to meet the requirements of finer films. Such routes are based on the Langmuir−Blodgett procedure,[5] self-assembly,[6,7] and two-dimensional sol−gel processes.[8]

Electrostatic self-assembly, or consecutive adsorption of oppositely charged polyelectrolytes, has advantages in terms of its high controllability of nanoarchitecture as well as thickness.[9] It is also characterized as being relatively simple, inexpensive, and less energy consuming. Several groups have applied this colloid self-assembly technique to produce multilayer ultrathin titania films,[7] in which titania nanoparticles are sequentially adsorbed with appropriate organic polyelectrolytes.

Apart from nanoparticles, unilamellar crystallites of titanium oxide, or a new type of nanosized semiconductor, have recently been obtained by exfoliating a layered titanate into individual colloidal sheets through soft-chemical treatment,[10] and their layer-by-layer assembly has been constructed by alternate adsorption with suitable polycations.[10a,11] The multi-

* Corresponding author. E-mail: sasaki.takayoshi@nims.go.jp. Fax: +81-298-54-9061.

(1) (a) Hagfeldt, A.; Grätzel, M. *Chem. Rev.* **1995**, *95*, 49. (b) Grätzel, M. Nanocrystalline Electronic Junctions. In *Semiconductor Nanoclusters: Physical, Chemical, and Catalytic Aspects*; Kumat, P. V., Meisel, D., Eds.; Elsevier: Amsterdam, 1996; Vol. 103, pp 353−375. (c) Kumat, P. V. *Native and Surface Modified Semiconductor Nanoclusters*; Kumat, P. V., Ed.; John Wiley & Sons: New York, 1997; Vol. 44, pp 273−343.

(2) (a) Jämting, Å. K.; Bell, J. M.; Swain, M. V.; Wielunski, L. S.; Clissold, R. *Thin Solid Films* **1998**, *332*, 189. (b) Lin, H.; Kozuka, H.; Yoko, T. *Thin Solid Films* **1998**, *315*, 111. (c) Mandelbaum, P. A.; Regazzoni, A. E.; Blesa, M. A.; Bilmes, S. A. *J. Phys. Chem. B* **1999**, *103*, 5505. (d) Yasumori, A.; Shinoda, H.; Kameshima, Y.; Hayashi, S.; Okada, K. *J. Mater. Chem.* **2001**, *11*, 1253.

(3) Chen, S.; Mason, M. G.; Gysling, H. J.; Paz-Pujalt, G. R.; Blanton, T. N.; Castro, T.; Chen, K. M.; Fictorie, C. P.; Gladfelter, W. L.; Franciosi, A.; Cohen, P. I.; Evans, J. F. *J. Vac. Sci. Technol.* **1993**, *A11*, 2419.

(4) (a) Mardare, D.; Tasca, M.; Delibas, M.; Rusu, G. I. *Appl. Surf. Sci.* **2000**, *156*, 200. (b) Remillard, J. T.; McBride, J. R.; Nietering, K. E.; Drews, A. R.; Zhang, X. *J. Phys. Chem. B* **2000**, *104*, 4440.

(5) (a) Kotov, N. A.; Meldrum, F. C.; Fendler, J. H. *J. Phys. Chem.* **1994**, *98*, 8827. (b) Doherty, S.; Fitzmaurice, D. *J. Phys. Chem.* **1996**, *100*, 10732. (c) Oswald, M.; Hessel, V.; Riedel, R. *Thin Solid Films* **1999**, *339*, 284.

(6) Rizza, R.; Fitzmaurice, D.; Hearne, S.; Hughes, G.; Spoto, G.; Ciliberto, E.; Kerp, H.; Schropp, R. *Chem. Mater.* **1997**, *9*, 2969.

(7) (a) Kotov, N. A.; Dékány, I.; Fendler, J. H. *J. Phys. Chem.* **1995**, *99*, 13065. (b) Liu, Y.; Wang, A.; Claus, R. *J. Phys. Chem. B* **1997**, *101*, 1385. (c) Kovtyukhova, N.; Ollivier, P. J.; Chizhik, S.; Dubravin, A.; Buzaneva, E.; Gorchinskiy, A.; Marchenko, A.; Smirnova, N. *Thin Solid Films* **1999**, *337*, 166. (d) Cassagneau, T.; Fendler, J. H.; Mallouk, T. E. *Langmuir* **2000**, *16*, 241.

(8) (a) Moriguchi, I.; Maeda, H.; Teraoka, Y.; Kagawa, S. *J. Am. Chem. Soc.* **1995**, *117*, 1139. (b) Moriguchi, I.; Maeda, H.; Teraoka, Y.; Kagawa, S. *Chem. Mater.* **1997**, *9*, 1050. (c) Ichinose, I.; Kawakami, T.; Kunitake, T. *Adv. Mater.* **1998**, *10*, 535.

(9) (a) Decher, G. Layered Nanoarchitectures via Directed Assembly of Anionic and Cationic Molecules. In *Comprehensive Supramolecular Chemistry, "Templating, Self-Assembly and Self-Organization"*; Sauvage, J. P., Hosseini, M. W., Eds.; Pergamon Press: Oxford, 1996; Vol. 9, pp 507−528. (b) Decher, G. *Science* **1997**, *277*, 1232.

10.1021/cm0202456 CCC: $22.00 © 2002 American Chemical Society
Published on Web 07/25/2002

layer ultrathin films obtained exhibit interesting properties, for example, intensive UV-absorption, which is associated with the novel features of the titania nanosheets, differing significantly from the properties of titania nanoparticles.[12]

It is of considerable importance and interest to further explore the modification of self-assembled titania ultrathin films. If these multilayer films can be converted into polymer-free inorganic films, it may open a new route for the design of new nanostructured films, appending significant importance to this self-assembly approach. Furthermore, such modification is expected to lead to new or enhanced properties, for example, improved chemical and mechanical stability. Because the internal structure, composition, and thickness of the films are highly defined on a nanometer scale, the obtained films may promote deeper understanding of properties such as catalytic activities that are highly surface-dependent. In the present study, we examine the effects of heat treatment and UV irradiation on a self-assembled multilayer film consisting of titania nanosheets and polycations. A variety of films are derived, and their physicochemical properties are studied.

Experimental Section

Reagents. All chemicals were of >99.9% purity or of analytical grade. Polyethylenimine (PEI, $M_w = \sim 7.5 \times 10^5$) and poly(diallyldimethylammonium (PDDA, $M_w = 1 \times 10^5$ to 2×10^5) chloride) were obtained from Aldrich Co. and used without further purification. Ultrapure water, filtered by a Milli-Q reagent water system to a resistivity of >17 MΩ cm, was used throughout the experiments.

Materials. Titania nanosheets of composition $Ti_{1-\delta}O_2^{4\delta-}$ ($\delta \sim 0.09$) were synthesized by delaminating a layered protonic titanate with γ-FeOOH structure into colloidal single layers according to procedures described previously: Briefly, a stoichiometric mixture of Cs_2CO_3 and TiO_2 was calcined at 800 °C for 20 h to produce a precursor cesium titanate, $Cs_{0.7}Ti_{1.825}\square_{0.175}O_4$ (□: vacancy),[13] about 70 g of which was treated with 2 dm^3 of a 1 mol dm^{-3} HCl solution at room temperature. This acid leaching was repeated three times by renewing the acid solution every 24 h.[14] The resulting acid-exchanged product was filtered, washed with water, and air-dried.

The obtained protonic titanate, $H_{0.7}Ti_{1.825}\square_{0.175}O_4 \cdot H_2O$, was shaken vigorously with a 0.017 mol dm^{-3} tetrabutylammonium hydroxide solution at ambient temperature for 10 days.[10] The solution-to-solid ratio was adjusted to 250 cm^3 g^{-1}. This procedure yielded a stable colloidal suspension with an opalescent appearance. In our previous study,[12] we demonstrated that this suspension contains unilamellar crystallites of $Ti_{1-\delta}O_2^{4\delta-}$ ($\delta = 0.09$) in the form of titania nanosheets of ~1 nm in thickness and 0.1−1 μm in lateral size.

Fabrication of Multilayer Assembly Films. Substrates such as quartz glass platelets and silicon wafer chips (1×5 cm^2) were cleaned by immersion in baths of 1/1 methanol/HCl and concentrated H_2SO_4 for 30 min each. The substrates were then washed with a copious amount of ultrapure water and stored in water until use. The substrate surface was converted to cationic by being primed with a PEI solution (2.5 g dm^{-3}, pH = 9), immediately prior to film deposition.

The titania nanosheets and PDDA were assembled layer-by-layer from the colloidal suspension of $Ti_{1-\delta}O_2^{4\delta-}$ (0.08 g dm^{-3}, pH = 9) and a PDDA solution (20 g dm^{-3}, pH = 9), respectively.[11] The substrate was immersed in each solution for 20 min and then rinsed meticulously with water. The operations for nanosheet/PDDA deposition were repeated 10 times to synthesize a multilayer assembly composed of 10 layer pairs, $PEI/Ti_{1-\delta}O_2/(PDDA/Ti_{1-\delta}O_2)_9$.

A multilayer film of PDDA/montmorillonite sheets was prepared for comparison purposes in a similar manner using a colloidal suspension (0.3 g dm^{-3}, pH = 8.0) of Kunipia-F (Kunimine Kogyo).

Heat Treatment and UV Irradiation of Films. The multilayer films were heated in air in an electronic furnace at temperatures of 100−1000 °C. The temperature was raised from room temperature at a rate of 5 °C min^{-1}, and then the sample was held at the set temperature for 1 h and allowed to cool spontaneously.

A 500 W Xe lamp (XEF-501S San-ei Electric) was used for UV irradiation of films. Samples were placed at ~10 cm from the light source, corresponding to a UV intensity of approximately 1 mW cm^{-2} at $\lambda < 300$ nm, as determined with a spectroradiometer (USR-30 Ushio Denki).

Instrumentation. X-ray diffraction (XRD) data were collected using a Rigaku Rint 2000S powder diffractometer with graphite monochromatized Cu Kα radiation ($\lambda = 0.154\ 05$ nm).

A Digilab S-45 FT-IR spectrometer equipped with a liquid nitrogen cooled MCT detector was used to acquire vibrational spectra in transmission mode for films fabricated on a silicon wafer chip (5×6 cm^2). Samples were aligned at a Brewster angle of 75° with respect to the incident beam.

X-ray photoelectron spectra (XPS) were taken at a takeoff angle of 45° using a Physical Electronics XPS-5700 spectrometer with the Al Kα X-ray line (1486.6 eV). The probing size was 0.8 mm in diameter.

A Hitachi U-4000 spectrophotometer equipped with an integrating sphere detection system was employed to record UV−visible absorption spectra for films on quartz glass substrates.

Ellipsometric measurements were performed using a Jovin-Ybon UVISEL/DH10 spectroscopic ellipsometer equipped with a photoelastic modulator and a 75 W Xe lamp as a light source. Scan data were obtained over a wavelength range of 240−830 nm at a fixed incident angle of 75°. The parameters ψ and Δ in the equation $r_p/r_s = (\tan \psi)e^{i\Delta}$, where r_p and r_s are the complex amplitude reflection coefficients for p- and s-polarized light, respectively, were fitted using an appropriate model based on a modified film architecture. In the fitting process, the thicknesses of the multilayer components were refined using optical constants for the $Ti_{1-\delta}O_2^{4\delta-}$ nanosheet, PEI, and PDDA, determined as described previously.[11b]

The water contact angle on the film surface was measured using a contact angle meter (CA-XP Kyowa Kaimen Kagaku). Samples were exposed to UV light from a 500 W Xe lamp for various lengths of time, and the contact angle was determined to estimate the hydrophilicity.

Results and Discussion

Structural Changes upon Heat Treatment and UV Irradiation. Figures 1 and 2 show the changes in XRD patterns when the multilayer film of titania nanosheets and polycations was heated in air. The quartz glass substrate is responsible for the halo pattern

(10) (a) Sasaki, T. Novel Nanosheet Crystallites and Their Layer-by-Layer Assembly. In *Handbook of Polyelectrolytes and Their Applications*; Tripathy, S., Kumar, J., Nalwa, H. S., Eds.; American Scientific Publishers: Stevenson Ranch, 2002; Vol. 1, pp 241−263. (b) Sasaki, T.; Watanabe, M.; Hashizume, H.; Yamada, H.; Nakazawa, H. *J. Am. Chem. Soc.* **1996**, *118*, 8329. (c) Sasaki, T.; Watanabe, M. *J. Am. Chem. Soc.* **1998**, *120*, 4682.

(11) (a) Sasaki, T.; Ebina, Y.; Watanabe, M.; Decher, G. *Chem. Commun.* **2000**, 2163. (b) Sasaki, T.; Ebina, Y.; Tanaka, T.; Harada, M.; Watanabe, M.; Decher, G. *Chem. Mater.* **2001**, *13*, 4661.

(12) (a) Sasaki, T.; Watanabe, M. *J. Phys. Chem. B* **1997**, *101*, 10159. (b) Sasaki, T.; Ebina, Y.; Kitami, Y.; Watanabe, M.; Oikawa, T. *J. Phys. Chem. B* **2001**, *105*, 6116.

(13) (a) Hervieu, M.; Raveau, B. *Rev. Chim. Miner.* **1981**, *18*, 642. (b) Grey, I. E.; Li, C.; Madsen, I. C.; Watts, J. A. *J. Solid State Chem.* **1987**, *66*, 7.

(14) (a) Sasaki, T.; Komatsu, Y.; Fujiki, Y. *Chem. Commun.* **1991**, 817. (b) Sasaki, T.; Watanabe, M.; Michiue, Y.; Komatsu, Y.; Izumi, F.; Takenouchi, S. *Chem. Mater.* **1995**, *7*, 1001.

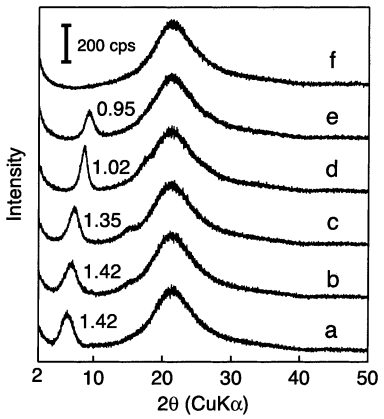

Figure 1. XRD patterns for a multilayer film of PDDA/$Ti_{1-\delta}O_2$ in the course of heat treatment: (a) as-deposited; (b) 100 °C; (c) 200 °C; (d) 300 °C; (e) 400 °C; (f) 500 °C. Numerals next to a diffraction peak denote the multilayer repeat distance in nm.

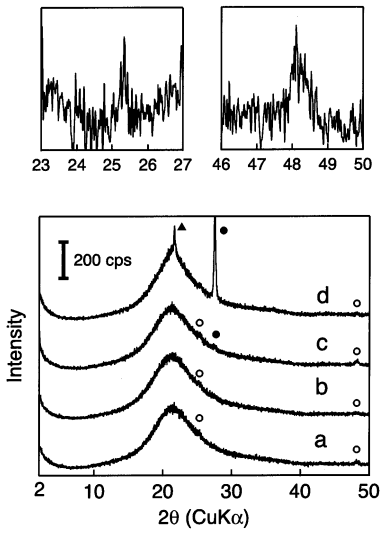

Figure 2. XRD patterns for a multilayer film of PDDA/$Ti_{1-\delta}O_2$ heated at (a) 600 °C, (b) 700 °C, (c) 800 °C, and (d) 900 °C. Open circles, closed circles, and triangles indicate the diffraction peaks attributable to anatase, rutile, and cristobalite (from substrate). Insets at the top are detailed patterns in a selected angular range of part a.

observed at a 2θ of 15−30°. The as-deposited film revealed a Bragg peak, arising from a repeating bilayer of PDDA/$Ti_{1-\delta}O_2$.[11] The multilayer repeat distance of 1.4 nm remained practically unchanged up to a heating temperature of 200 °C, indicating a negligible change in the film up to this temperature. This spacing was observed to contract to less than 1 nm between 200 and 400 °C, which should be attributable to the pyrolysis of organic species in the film. The inter-nanosheet shrinkage of 0.4−0.5 nm is consistent with the loss of PDDA.[11,15] To confirm this, we prepared a bulk sample of PDDA/$Ti_{1-\delta}O_2$ nanocomposite by direct addition of a PDDA solution to the titania nanosheet suspension, and carried out thermal analysis. A large weight loss was observed in the temperature range 260−500 °C, accompanied by a sharp exothermic peak. This thermal event can only be explained by the combustion of PDDA.

The multilayer nanostructure was stable up to 400 °C. However, the basal diffraction peak from the sample

(15) Glinel, K.; Laschewsky, A.; Jonas, A. M. *Macromolecules* **2001**, *34*, 5267.

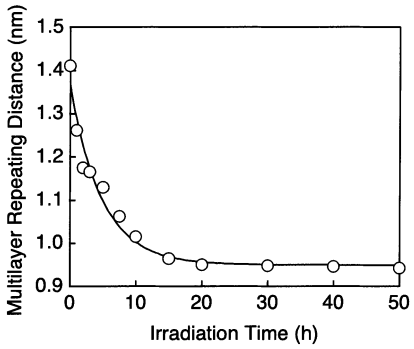

Figure 3. Multilayer repeat spacing as a function of UV-irradiation time.

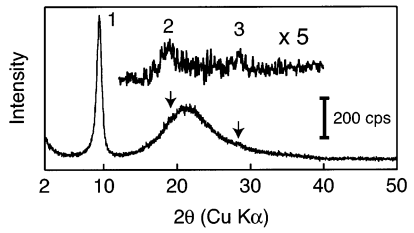

Figure 4. XRD pattern for a multilayer film exposed to UV light for 50 h. Numerals represent the order of the basal reflections. Arrows mark positions of second- and third-order lines, which are shown in the inset trace in a higher enlargement after baseline correction.

disappeared at 500 °C, indicative of the collapse of the multilayer. Anatase crystallized in its place at 600 °C and above, as revealed by 101 and 200 peaks that appeared around $2\theta = 25.4°$ and 48.0°, respectively. The faint signals may be attributable to the very small size of anatase crystallite as well as the small quantity of sample. Anatase transformed into rutile above 800 °C, as is generally observed for TiO_2. The diffraction peaks for rutile in the sample heated at 900 °C were much stronger than those for anatase in the samples formed at lower temperatures.

Apart from the thermal treatment, exposure of the multilayer film to UV light induced interesting effects. The multilayer repeat distance contracted continuously with irradiation time down to a constant value of 0.94 nm after 20 h (see Figure 3). The shrinkage upon UV-illumination is ascribed to decomposition of PDDA from the gallery, which is promoted via the photocatalytic activity of the titania nanosheet. In a control test, a multilayer film of PDDA/aluminosilicate (montmorillonite) sheets did not undergo contraction of the repeat distance (∼2.7 nm) under similar UV-illumination.

The UV-exposed sample possessed a well-ordered multilayer nanostructure. As shown in Figure 4, the intensity of the diffraction peak was enhanced by ∼4 times and the profile became much sharper when compared with that for the as-grown film. In addition, the higher-order basal reflections became detectable. One can notice a similar tendency for the film heat-treated at 300 °C (see Figure 1), although to a lesser extent. The improvement in crystallinity is explained by the removal of PDDA. The presence of polymer is expected to introduce fluctuations in the basal distance and misalignment of the nanosheet crystallites. In our previous study, we demonstrated that the multilayer repeat distance in the as-grown film has a standard deviation of ∼20% around an average value of 1.4 nm.[11b]

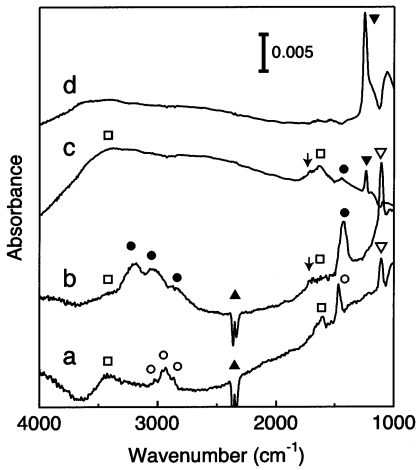

Figure 5. FT-IR spectra for the films: (a) as-deposited; (b) UV-irradiated; (c) heated at 400 °C; (d) heated at 600 °C. Open circles, closed circles, and open squares represent absorption bands attributable to PDDA, NH_4^+, and H_2O (H_3O^+), respectively. Closed triangles and open and closed inverted triangles denote peaks assigned to gaseous CO_2, the surface oxide of Si−O−Si, and the alkyl group bound to the substrate, respectively.

Characterization by FT-IR and X-ray Photoelectron Spectroscopy. The films were analyzed by FT-IR spectroscopy (see Figure 5) in order to obtain a full understanding of the changes induced in the multilayer film by heat treatment and UV irradiation. The as-deposited film exhibited absorption bands characteristic of polycations: sharp peaks at 3020, 2961, 2932, and 2864 cm^{-1} attributable to the stretching modes of $-CH_3$ and $-CH_2-$.[16] A corresponding bending vibration was also detected at 1472 cm^{-1}. Broad bands at 3600−3000 and ∼1620 cm^{-1} are assignable to the stretching and bending vibrations of H_2O or H_3O^+,[16] indicating that the film is hydrated. The sharp band at 1107 cm^{-1} may be ascribed to the Si−O−Si stretching frequency, which is from the surface oxide of the silicon wafer substrate.[16]

The spectra for the heat-treated and UV-exposed films were very different from those of the as-grown film. The absorption bands attributable to organic polymers completely disappeared, and the UV-irradiated sample exhibited three broad peaks in the range 3300−2800 cm^{-1} and a relatively sharp peak at 1427 cm^{-1}. These bands clearly indicate the formation of NH_4^+. The former three can be assigned as N−H stretching vibrations in NH_4^+, and the latter as its bending mode.[16] Besides these major peaks, weak absorptions from H_2O or H_3O^+ were also detected.

The formation of NH_4^+ upon UV-illumination is reasonably understood as the result of photocatalytic splitting of PDDA, which bears quaternary ammonium groups. As recently demonstrated, NO_3^- and NH_4^+ are the most usual final products in the photocatalytic degradation of amines.[17] However, NO_3^- may not be preferred in this case, because the titania nanosheets are negatively charged. Cationic species are required to maintain the total charge neutrality of the system. Actually, there was no absorption band in the wavenumber range 1410−1340 cm^{-1}, where a strong peak for NO_3^- is expected to occur.[16]

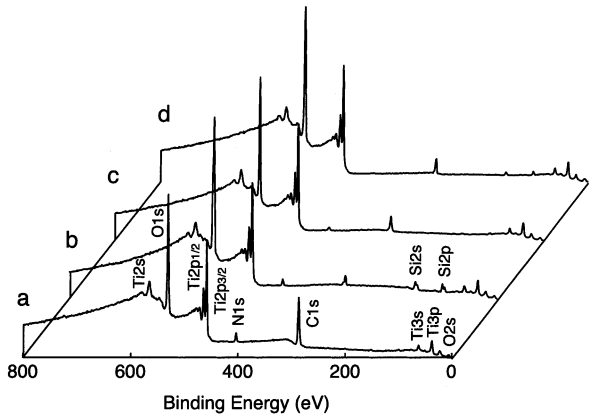

Figure 6. Survey XPS data for the films: (a) as-deposited; (b) UV-irradiated; (c) heated at 400 °C; (d) heated at 600 °C.

In contrast, the sample heated at 400 °C had absorption peaks attributable to H_2O or H_3O^+ as major spectral features. The presence of NH_4^+ is also suggested by a peak at 1427 cm^{-1}, which may be attributable to deformative vibration of N−H bonds. Signals arising from N−H stretching modes (3300−2800 cm^{-1}) were not clearly detected, possibly because of their broad nature as well as the low yield. We speculate that the charge neutrality is achieved by protons, most likely in the form of H_3O^+, as well as by NH_4^+. A faint signal at 1710 cm^{-1} was also discernible (indicated by an arrow in Figure 5), implying the existence of a saturated aliphatic carboxylic acid or related group.[16] The UV-irradiated film showed a similar feature. Its origin will be discussed later with XPS data. Another noteworthy aspect is loss of the signal at 1107 cm^{-1} and appearance of a new peak at 1250 cm^{-1}. The latter band may be due to vibration of Si−R bonds (R: alkyl group),[16] suggesting that the substrate surface was modified during the combustion of polycations.

The film heated at 600 °C is composed of TiO_2 (anatase), as described above. The IR data for this film was rather featureless except for faint signals from a trace amount of H_2O. This is reasonable considering that no further cationic species are necessary because of the loss of the negatively charged nanosheets.

XPS data provide detailed and complimentary information on modifications of the film (see Figure 6). A spectrum of the as-prepared film gave major peaks assignable to Ti, O, C, and N, supporting that the multilayer assembly is composed of titania nanosheets and an organic polycation such as PDDA. The $2p_{3/2}$ and $2p_{1/2}$ core levels of Ti occurred at 458.8 ± 0.2 and 464.4 ± 0.2 eV, respectively, which agrees well with the binding energies for TiO_2 in the literature.[18] The absence of energy deviations suggests that charging of the samples could be ignored. The O(1s) peak was detected at a binding energy of 530.4 ± 0.2 eV in all

(16) (a) Socrates, G. *Infrared Characteristic Group Frequencies*; 2nd ed.; John Wiley & Sons: Chichester, 1994. (b) Moenke, H. H. W. *The Infrared Spectra of Minerals*; Farmer, V. C., Ed.; Mineralogical Society: London, 1974, pp 365−382.

(17) (a) Klare, M.; Scheen, J.; Vogelsang, K.; Jacobs, H.; Broekaert, J. A. C. *Chemosphere* **2000**, *41*, 353. (b) Horikoshi, S.; Watanabe, N.; Mukae, M.; Hidaka, H.; Serpone, N. *New J. Chem.* **2001**, *25*, 999.

(18) (a) Moulder, J.; Stickle, W.; Sobol, P.; Bomben, K. *Handbook of X-ray Photoelectron Spectroscopy*; Chastrain, J., Ed.; Perkin-Elmer Corp.: Eden Prairie, 1992. (b) *NIST X-ray Photoelectron Spectroscopy Database*; The U.S. Secretary of Commerce, 1997.

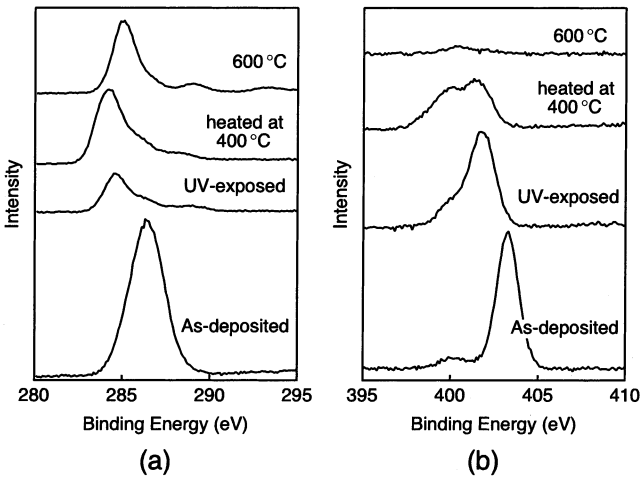

Figure 7. High-resolution scan for XPS (a) C(1s) and (b) N(1s) peaks.

Table 1. Atomic Ratio Estimated from XPS Analysis[a]

film	C	N	Ti	O[b]
as-grown	2.38	0.23	0.9125	2.04
UV irradiat	0.49	0.18	0.9125	1.89
heated at 400 °C	0.76	0.11	0.9125	1.98
heated at 600 °C	0.62	0.02	0.9125	1.84

[a] Normalized to a Ti content of 0.9125 in the chemical formula of nanosheet crystallite $Ti_{1-\delta}O_2$ ($\delta = 0.0875$). [b] O populations for the UV-exposed film and the film heated at 600 °C were obtained from the peak at 530.0 eV by separating the contribution at 532.5 eV due to SiO_2 at a substrate surface. Note that peaks attributable to silicon were detected for these samples (see Figure 6).

samples, which is characteristic of O bound to Ti.[18] In contrast, the relative intensity and chemical shift of C(1s) and N(1s) peaks were dependent on the film specifications, as displayed in Figure 7.

Table 1 lists the elemental ratios obtained from the XPS data. It should be noted that the accuracy of this quantification is not perfectly reliable for several reasons, primarily that XPS analysis does not always provide chemical composition data for an entire system because of its surface sensitivity. However, the compositional data in Table 1 are still useful. All films were found to have a Ti/O ratio close to the stoichiometry of the nanosheet (=0.9125/2), demonstrating the validity of this analysis.

The C/N ratio in the as-grown film was a little larger than the expected value of 8 for PDDA. This may be due to hydrocarbons of low-molecular weight, which easily adsorb onto sample surfaces. It is known that the XPS signal from C is often perturbed for this reason because of its surface sensitivity.[19] If we take the *N* value as the ground for a polycation content, the multilayer assembly accommodates ~0.2 mol of PDDA per formula weight. This agrees well with the composition of the bulk PDDA/$Ti_{1-\delta}O_2$ nanocomposite prepared as described above. The N content remains almost unchanged after UV exposure whereas the C content drops remarkably. In contrast, the loss of N as well as C was evident after heat treatment.

The C(1s) and N(1s) peaks for the as-grown sample were present at 286.3 and 403.3 eV, respectively, and are assigned to aliphatic chains and quaternary ammonium groups in PDDA. Upon heat treatment and UV irradiation, the main C peak shifted to a lower binding energy of 284−285 eV accompanied by evolution of a small peak around 289 eV. The former may be attributable to hydrocarbons of low molecular weight, and the latter is consistent with the characteristic peak location of −COOH. The C signals may not all necessarily be due to residual organic substances inside the multilayer assemblies. A similar XPS signal has been frequently observed for various samples, and this has been ascribed to contamination.[19] We also attribute the C signals observed in the heated samples and UV-irradiated film to adsorbed hydrocarbons. As described above, the as-grown film shows the C/N ratio of ~10, which is higher than the theoretical value of 8 for PDDA. If the excess is taken as a C contamination, its amount is comparable to those found for the heat-treated films and UV-irradiated sample.

The N(1s) peak also exhibited a marked difference from that in the as-deposited film. The resolved peak apparently indicates two components, the binding energies of which are 400 and 401.5 eV. The component having the higher binding energy was dominant in the UV-exposed film, whereas the two components were comparable in the sample heated at 400 °C. The peak at 401.5 eV agrees with the chemical shift for NH_4^+,[18] being consistent with the vibrational spectra described above. Absence of NO_3^- is confirmed again because it is expected at a higher binding energy of 406−408 eV.[18] It is difficult to determine from these data the chemical species responsible for the peak with lower binding energy. The literature indicates that various substances such as NH_3, CH_3CN, and $N_2H_4^{2+}$ can give a binding energy in this range.[18]

To sum up all the characterization data above, we can conclude that heat treatment at 400 °C or exposure to UV eliminates PDDA from the nanosheet gallery, yielding inorganic layered assemblies having small cationic species such as H_3O^+ and NH_4^+. This is further supported by ellipsometric thickness data, as will be described below. The resulting polycation-free multilayer assemblies are comparable to the precursor protonic titanate, $H_{0.7}Ti_{1.825}\square_{0.175}O_4 \cdot H_2O$, and its ammonium ion-exchanged phase, $(NH_4)_{0.4}H_{0.3}Ti_{1.825}\square_{0.175}O_4 \cdot 0.85H_2O$. More precisely, the UV-exposed film may be very close to the ammonium ion-exchanged phase, whereas the film heated at 400 °C may be intermediate between these two phases. The gallery heights of these bulk materials, 0.94 and 0.92 nm, were similar to those found for the modified films, although the body-centered layer sequence was lost in the multilayer films. Furthermore, the vibrational spectra for these materials are nearly coincident with those for the films (refer to the previously reported data[14] and the Supporting Information).

Optical Properties. Figure 8 shows UV−visible absorption spectra over the course of heating. The as-deposited film exhibited a sharp and intense absorption peak at 265 nm, which is characteristic of the molecular titania nanosheet having a high molar extinction coefficient, $\epsilon = 1.2 \times 10^4$ mol^{-1} dm^3 cm^{-1} at 265 nm.[11b,12a] The spectral profile remained almost unchanged up to 400 °C, while broadening was observed at 500 °C with

(19) Swift, P.; Shuttleworth, D.; Seah, M. P. *Practical Surface Analysis by Auger and X-ray Photoelectron Spectroscopy;* Briggs, D., Seah, M. P., Eds.; John Wiley & Sons: Chichester, 1983.

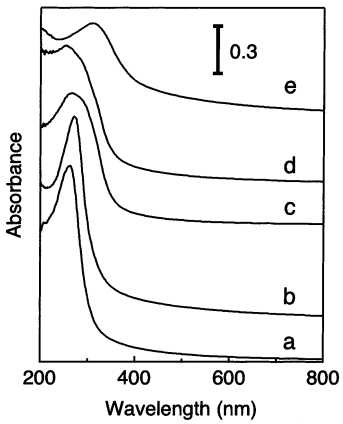

Figure 8. UV−visible absorption spectra for films in the heating process: (a) As-deposited; (b) 400 °C; (c) 500 °C; (d) 800 °C; (e) 900 °C.

Table 2. Ellipsometric Analysis Results

	thickness (nm)		
film	$Ti_{1-\delta}O_2$ layer	PDDA layer	total
as-grown	1.19	0.67	18.6
UV-irradiated	1.25	0.07	13.2
heated at 400 °C	1.12	0.0	11.2
heated at 600 °C			11.4

an accompanying red-shift of the absorption edge and reduction in intensity. This drastic change coincides with the phase transformation from two-dimensional nanosheet crystallites to anatase. In fact, the spectra for 500 °C and above are similar to those reported for nanocrystalline anatase. Another noticeable change took place at 900 °C, resulting in a spectral profile characteristic of bulk rutile. The formation of bulk rutile may be compatible with the sharp diffraction peak in the XRD pattern, as well as the change in the visible appearance of the film from transparent to semitransparent.

In contrast, no apparent change in UV−visible spectra was observed for the film exposed to UV light. This is in accordance with the experimental data above; the nanosheet crystallite itself did not change upon UV-illumination.

Figure 9 shows the refractive index and extinction coefficient for the films, as deduced by spectroscopic ellipsometry. The optical constant data are dependent on the film composition and structure, with a tendency to remain virtually consistent with the UV−visible spectra above. As detailed before,[11] the ellipsometric scan data for the as-deposited films were fitted on a multilayer model of alternating layers of the titania nanosheet and PDDA, giving layer thicknesses of 1.19 and 0.67 nm, respectively. As there are 10 layer pairs, the total film thickness is 18.6 nm.

Similar fitting of scan data for a film heated at 400 °C and a film exposed to UV light revealed that the thickness of PDDA layers was nearly negligible in these films, whereas the thickness of the $Ti_{1-\delta}O_2$ layers remained virtually unchanged (see Table 2). This is consistent with the conclusion that the polymer is removed by the treatments. The data for the film heated at 600 °C were analyzed by one medium model because the multilayer structure was lost at this temperature. The observed decreases in total film thickness upon heat

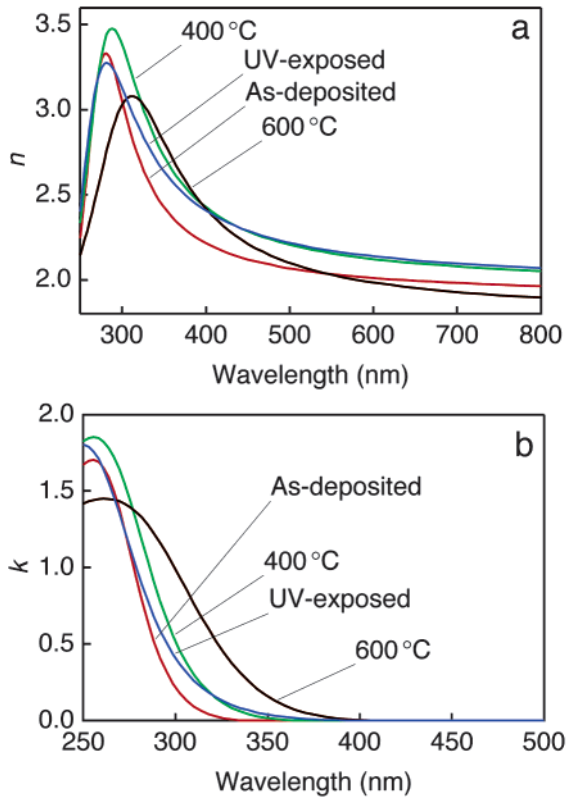

Figure 9. Optical constants of the films as a function of wavelength.

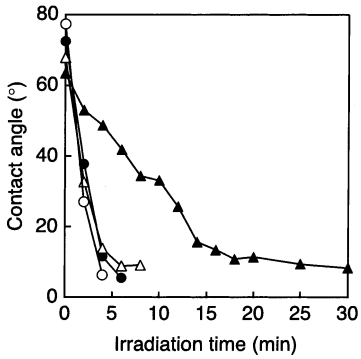

Figure 10. Contact angle of a water droplet as a function of UV-illumination time. Filled triangles, open circles, filled circles, and open triangles designate data for a PDDA/$Ti_{1-\delta}O_2$ nanocomposite film and polymer-free films synthesized from it by UV-irradiation and heat treatment at 400 and 600 °C, respectively.

treatment and exposure to UV light correspond to 39% and 29% of the total thickness of the as-deposited film, respectively. This is in good agreement with the XRD data, which indicated ∼34% shrinkage in the multilayer repeat spacing.

Photoinduced Hydrophilicity. The film surface became hydrophilic upon exposure to white light from the Xe lamp, as depicted in Figure 10. The hydrophilic conversion rate was dependent on the film specifications. The contact angle decreased to 5° or below for the polymer-free films after irradiation for 5 min. The UV-irradiated film exhibited the highest conversion rate among the three inorganic films. In contrast, the as-grown nanocomposite film exhibited hydrophilicity after irradiation for longer than 15 min. The presence

of PDDA is apparently responsible for this difference. These data suggest that photoinduced hydrophilicity can be controlled, depending on the composition and structure of the films.

The photoinduced hydrophilic conversion of TiO_2 surfaces has been studied extensively since its discovery in 1997.[20] The mechanism is presently under debate, with the main controversy associated with the surface structure of TiO_2.[21] The titania nanosheet has an atomic arrangement of γ-FeOOH type, and its (010) plane should lie exclusively parallel to the substrate surface. Although its atomic architecture differs from that of the crystal surfaces of anatase or rutile, the hydrophilic conversion rate was comparable to that for films of polycrystalline anatase. The present data may throw light upon the hydrophilic conversion mechanism, and a detailed study is currently underway.

(20) Wang, R.; Hashimoto, K.; Fujishima, A.; Chikuni, M.; Kojima, E.; Kitamura, A.; Shimohigoshi, M.; Watanabe, T. *Nature* **1997**, *388*, 431.

(21) Sakai, N.; Fujishima, A.; Watanabe, T.; Hashimoto, K. *J. Phys. Chem. B* **2001**, *105*, 3023.

Acknowledgment. The authors are grateful to Mr. Y. Yajima of National Institute for Materials Science for his assistance with wet chemical analysis.

Supporting Information Available: XRD and FT-IR data for the ammonium ion-exchanged titanate (PDF). The phase was synthesized by reacting a cesium titanate, $Cs_{0.7}Ti_{1.825}\square_{0.175}O_4$, with molten NH_4NO_3 at 200 °C for 3 days. After cooling to room temperature, the product was recovered by dissolving excess NH_4NO_3 with water. Chemical analysis indicated a composition of $(NH_4)_{0.39}H_{0.31}Ti_{1.825}\square_{0.175}O_4 \cdot 0.85H_2O$ (Calcd: TiO_2, 83.8%; N, 3.14%; ignition loss, 16.2%. Found: TiO_2, 83.9%; N, 3.17%; ignition loss, 16.0%).[22] This material is available free of charge via the Internet at http://pubs.acs.org.

CM0202456

(22) Elemental analysis was carried out as follows. Titanium. A weighed amount of the nanocomposite was dissolved with a H_2SO_4/HF solution. The Ti content was obtained gravimetrically as TiO_2 by precipitation of Ti cupfferon complex and its subsequent calcination at 1000 °C. Nitrogen: The sample was fused with NaOH pellets (~3 g) under a moist air flow, converting constituent N into NH_3. The NH_3 gas was absorbed into a H_3BO_3 solution, which was volumetrically titrated with a standard H_2SO_4 solution. Ignition loss: A weight loss was obtained by heating the sample at 1000 °C for 1 h.